Optimizing the Flexural Strength of Beams Reinforced with Fiber Reinforced Polymer Bars Using Back-Propagation Neural Networks

Bahman O. Taha[1], Peshawa J. Muhammad Ali[2] and Haval A. Ahmed[2]

[1]Department of Civil Engineering, Erbil Technical Engineering College
Erbil, Kurdistan Region - F.R. Iraq

[2]Department of Software Engineering, Koya University
Daniel Mitterrand Boulevard, Koya KOY45, Kurdistan Region - F.R. Iraq

Abstract—The reinforced concrete with fiber reinforced polymer (FRP) bars (carbon, aramid, basalt and glass) is used in places where a high ratio of strength to weight is required and corrosion is not acceptable. Behavior of structural members using (FRP) bars is hard to be modeled using traditional methods because of the high non-linearity relationship among factors influencing the strength of structural members. Back-propagation neural network is a very effective method for modeling such complicated relationships. In this paper, back-propagation neural network is used for modeling the flexural behavior of beams reinforced with (FRP) bars. 101 samples of beams reinforced with fiber bars were collected from literatures. Five important factors are taken in consideration for predicting the strength of beams. Two models of Multilayer Perceptron (MLP) are created, first with single-hidden layer and the second with two-hidden layers. The two-hidden layer model showed better accuracy ratio than the single-hidden layer model. Parametric study has been done for two-hidden layer model only. Equations are derived to be used instead of the model and the importance of input factors is determined. Results showed that the neural network is successful in modeling the behavior of concrete beams reinforced with different types of (FRP) bars.

Index Terms—Concrete, fiber reinforced bars, fiber reinforced polymer (FRP), neural networks.

I. INTRODUCTION

Fiber-reinforced polymers (FRP) are composite materials which made of fibers embedded in a polymeric resin. FRP has become an alternative to steel reinforcement for concrete

structures. Since FRP materials are nonmagnetic and noncorrosive, the problems of electromagnetic interference and steel corrosion can be avoided using FRP reinforcement. FRP materials have a high tensile strength which makes them suitable for use as a structural reinforcement. The anti-corrosion characteristic of FRP concretes is useful for structures in marine environments, in chemical and other industrial plants, in places where good quality concrete cannot be achieved and in thin structural elements.

The mechanical behavior of FRP reinforcement differs from the behavior of steel reinforcement. FRP materials are anisotropic and are characterized by high tensile strength only in the direction of the reinforcing fibers. FRP materials do not exhibit yielding; rather, they are elastic until failure. Design procedures should account for a lack of ductility in a concrete reinforced with FRP bar.

The neural network is a technique that can be used in modeling complicated and interrelated data. It simulates the way that human's brain works. Multilayer Perceptron (MLP) is a feed forward neural network, which can be used successfully in prediction and modeling. The neural network can learn from collected data only, without any prior knowledge about the nature of the relationships among factors. A supervised learning can be conducted by comparing the output with the target, the difference is propagated back to update all connecting links between nodes, this algorithm is called back-propagation. Neurons are arranged in layers, input, hidden layer(s) and output layer.

Experimental studies have been done in evaluating the flexure strength and behavior of concrete beams reinforced with different types of FPR bars having different concrete compressive strengths (Taha, 2013; Al-Shamaa, 2010; Chitsazan, et al., 2010; Barris, et al., 2009; Al-Sunna, 2006). Also, neural networks technique is used to predict the behavior of existing beams strengthened with FRP sheets (Leung, et al., 2006; Yousif and Al-Jurmaa, 2010; Mashrei, et al., 2013). Many other studies have been done in predicting the behavior of concrete members in shear reinforced with or strengthened with FRP (Perera, et al., 2014; Metwally, 2013;

Lee and Lee, 2014). The aim of this work is to modeling concrete beams in flexure reinforced with fiber polymer bars using back-propagation neural networks.

The objectives of this research work are;
1) Constructing and training the model on the collected data.
2) Using the model for predicting the flexural strength of concrete beams reinforced with FRP bars.
3) Writing mathematical equations to represent the model.
4) Determining the relative importance of input factors.
5) Doing a parametric study for major parameters that affect the flexural strength of high strength concrete beams.

For this purpose a number of high strength concrete beams reinforced with carbon and glass fibers were predicted taking different parameters into account. The parameters include; the effect of the effective depth (d), concrete compressive strength ($f'c$), and the flexural reinforcement ratio (ρ). The rest of the paper is organized as follows: Section II presents the neural network model, Section III presents the weights equations, Section IV shows the importance of input factors and parametric study is presented in Section V. Finally, Section VI concludes the paper.

II. The Neural Network Model and the Experimental Results

The system includes five phases: data collection, preprocessing, creation of the model, learning, and evaluation of the model. The system can be illustrated in the process diagram shown in the Fig. 1.
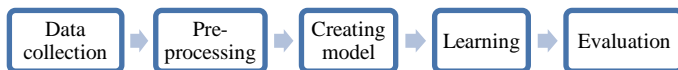
Fig. 1. Process diagram of the system.

A. Data Collection

Data are collected from different published papers, where different types of fiber reinforced polymer bars are used (carbon, aramid, basalt and glass). Most of researches done previously have been working on one specific type of fiber polymer bars, whereas, in this paper different types of fiber polymers are collected, therefore, the model can be used to predict the flexural strength of beams reinforced with all types of fiber polymer bars. Five important factors which influencing the strength of a beam in flexure are taken in consideration. Factors are, the width of the beam (b), the effective depth of the beam (d), cylindrical concrete compression strength ($f'c$), the ultimate tensile strength of fiber reinforced polymer bars (fu), and reinforcement ratio (ρ), the empirical moments capacity are used as target data. 101 samples were collected from nine sources (Taha, 2013; Al-Shamaa, 2010; Chitsazan, et al., 2010; Barris, et al., 2009; Al-Sunna, 2006; Toutanji and Saafi, 2000; Masmoudi, et al., 1998; Duranovic, et al., 1997; Benmoktane, et al., 1995), the collected data are arranged in Appendix A. The ranges of the collected data and measurement units are given in Table I.

TABLE I
INFLUENCED FACTORS, RANGES OF DATA AND MEASUREMENT UNITS

Factors and empirical strength	Unit	Minimum	Maximum
Width of the beam (b)	mm	80	500
Effective depth of the beam (d)	mm	70.48	509.00
Concrete compression strength ($f'c$)	MPa	31.20	100.82
Bars ultimate tensile strength (fu)	MPa	600	2300
Reinforcement ratio % (ρ)	----	0.15	4.05
Empirical moment caused the failure (Mu)	KN.m	5.43	181.70

B. Data Preprocessing

In this paper, Weka package (Hall, et al., 2009) is used for creating and learning the model. Weka is a software that can be used for all purposes of data mining and knowledge extraction. It provides a very easy to use and friendly environment. The package is imported to a self-created Java program and used for creating and learning the model. Using this package enables the user to specify the structure of the model like number of hidden layers and the number of nodes inside each layer and type of the transfer functions for each layer. Weka uses a random initialization for weights and bias values.

To minimize the bias of one feature over another, data normalization is necessary. This step has been done automatically by the Weka package which makes the input features within the same range of values. In this paper min-max [-1, +1] normalization is used which casts all features to the range [-1, +1].

C. Creating Models

In this paper, two models of MLP Neural Network are created. The first model was created with three layers: an input, a hidden layer and an output layer. The structure can be summarized as BPNN1(5-3-1), shown in the Fig. 2. The second model consists of input, two hidden layers and an output layer BPNN2(5-5-3-1), the structure of the second model is shown in Fig. 3. All activation functions of hidden layers for both models are sigmoid functions while the activation function of the output layer is a linear function. Notice that the word "layer" hasn't been appended to the word "input". This is because the input is not a real layer where there is no summation, no bias, and no transfer function (Muhammad Ali, et al., 2013; Muhammad Ali, 2014).

Choosing number of hidden layers and number of nodes in each layer depends on different factors. It depends on the complexity of the problem, the size of the training data set dealing with and the quality of the data. Usually, the number of nodes in the hidden layer is ranging between the number of nodes in the input and the number of the nodes in the output layer. To find a suitable structure of the neural model, different structures should be tested then the best can be selected.

D. Learning Process

The back-propagation is used for supervised learning. In this method, an artificial network learns from computing the error between the output values with target values, then

propagating back this error by justifying the weights of the connections between nodes. This backward-propagation of errors needs the transfer functions used in the nodes to be differentiable to ensure a smooth back-distribution of errors on the weights. Gradient descent with moment (GDM) algorithm is used for back-propagation. The detail of the learning process for both models is shown in Table II.
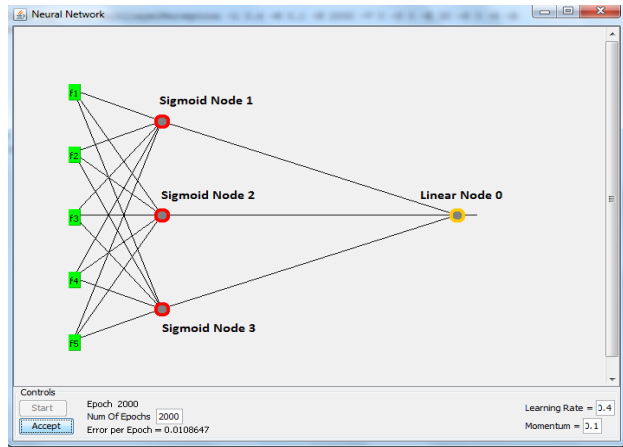
Fig. 2. The neural network model BPNN1(5-3-1).
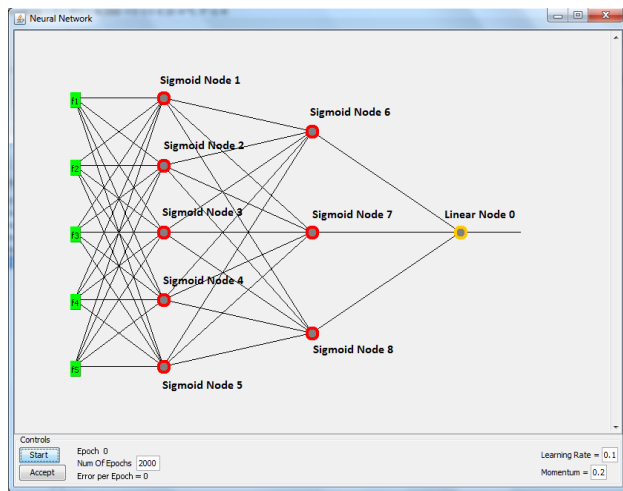
Fig. 3. The neural network model BPNN2(5-5-3-1).

TABLE II
LEARNING PROCESS DETAILS

Parameters	BPNN1(5-3-1)	BPNN2(5-5-3-1)
Learning rate	0.4	0.1
Momentum	0.1	0.2
Epoch	2000	2000

E. Evaluation

The 101 collected samples were divided into two parts, 91 of them (90%) were used for training the neural network models, and the other 10 items (10%) were used for testing. These 10 unseen data are used for finding the correlation of the model with the actual observed results. The results showed

that the BPNN2(5-5-3-1) model (R=0.9832) is better correlated than the first structure. Therefore, the second model is used. Fig. 4 shows the correlation between predicted data and actual data for BPNN1(5-3-1), and Fig. 5 shows the same correlation for BPNN2(5-5-3-1) model.
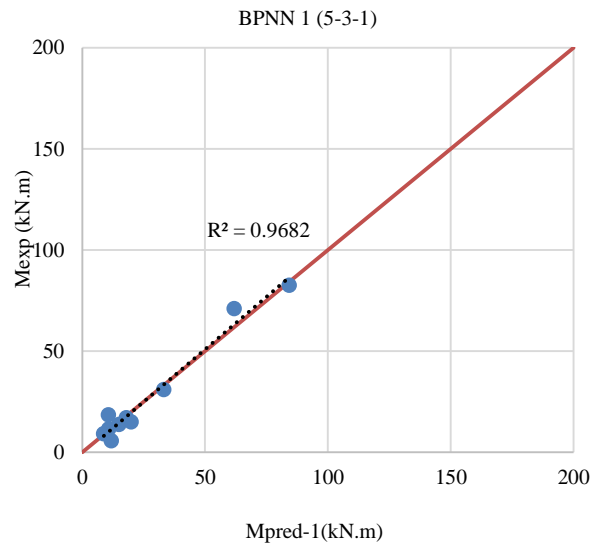
Fig. 4. The correlation between actual and predicted data for BPNN1 (test set only).
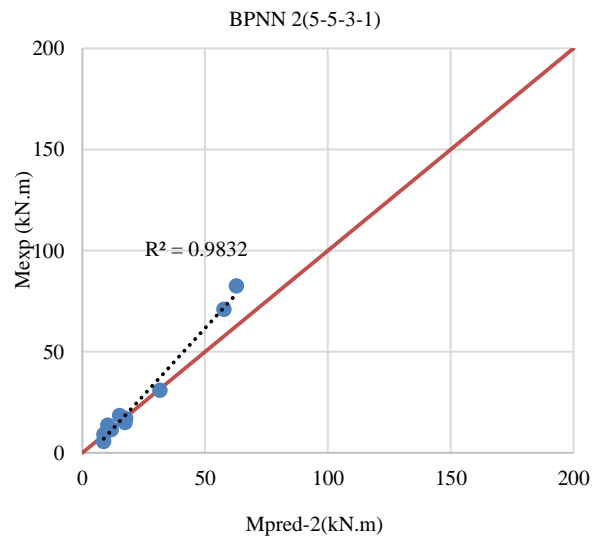
Fig. 5. The correlation between actual and predicted data for BPNN2 (test set only).

III. WEIGHTS AND EQUATIONS

The neural network model can be mathematically represented by one mathematical equation, but for the sake of simplicity, it's better to present the model in several simpler equations, especially for models have more than one hidden layer. In this section, the BPNN2 model is presented in (1) to (8). The min-max normalization is necessary to bring all features to the range [-1, +1] to eliminate the influence of one feature over another feature.

$$x' = 2*\left[\frac{x-min}{max-min}\right]-1 \qquad (1)$$

Where x' is the normalized values, x is the value before normalizing, min and max are minimum and maximum values of any feature shown in Table I.

$$A = \frac{1}{1+e^{\left[-1.9+0.1(b)+1.2(d)-2.4(fc)-0.02(fu)+3.1(r)\right]}} \qquad (2)$$

$$B = \frac{1}{1+e^{\left[1.2-0.9(b)-4.5(d)+0.5(fc)-0.02(fu)-0.1(r)\right]}} \qquad (3)$$

$$C = \frac{1}{1+e^{\left[0.6-0.2(b)-1.5(d)+0.4(fc)-0.7(fu)-0.5(r)\right]}} \qquad (4)$$

$$D = \frac{1}{1+e^{\left[-1.9-0.1(b)-2.5(d)-0.7(fc)+0.5(fu)-3.96(r)\right]}} \qquad (5)$$

$$E = \frac{1}{1+e^{\left[0.7-0.3(b)-1.6(d)+0.1(fc)-0.6(fu)-0.4(r)\right]}} \qquad (6)$$

Where b is the width of the beam in mm, d is the effective depth in mm, fc is the concrete compression strength in MPa, fu is bars' ultimate tensile strength in MPa, and r is reinforcement ratio in %. e is the exponential function and other constant numbers are the weights of the trained model. A, B, C, D, and E are calculated and inserted to (7):

$$y' = 1.129 - \frac{1.755}{1+e^{\left[-0.36+1.39 A+1.70 B+0.51 C+D+0.30 E\right]}} - \frac{2.099}{1+e^{\left[-1.68+1.32 A+2.09 B+0.50 C+1.68 D+0.30 E\right]}} - \frac{1.765}{1+e^{\left[-0.43+1.35 A+1.66 B+0.45 C+1.09 D+0.28 E\right]}} \qquad (7)$$

$$M = \left[\left(\frac{y'+1}{2}\right)(max-min)\right]+min \qquad (8)$$

Where y' is the output of the model before denormalizing, M is the moment capacity in KN.m, min and max are the minimum and maximum values of target feature before normalization.

IV. IMPORTANCE FACTOR

The relative importance study for input factors has been done based on the importance of weights using the method proposed by (Garson, 1991), see (9).

$$I_j = \frac{\sum_{m=1}^{m=Nh}\left(\left(\frac{|W_{jm}^{ih}|}{\sum_{k=1}^{Ni}|W_{km}^{ih}|}\right)\times|W_{mn}^{ho}|\right)}{\sum_{k=1}^{k=Ni}\left\{\sum_{m=1}^{m=Nh}\left(\left(\frac{|W_{jm}^{ih}|}{\sum_{k=1}^{Ni}|W_{km}^{ih}|}\right)\times|W_{mn}^{ho}|\right)\right\}} \qquad (9)$$

Where, I_j is the relative importance of the jth input variable on the output variable, Ni and Nh are the numbers of input and hidden neurons, respectively, W is connection weights, the superscripts "i", "h" and "o" refer to input, hidden and output layers, respectively, and subscripts "k", "m" and "n" refer to input, hidden and output neurons, respectively. Table III shows the relative importance ratio for both models calculated according to Garson's method.

It's clear that in both models the effective depth (d) has the greatest influence on the moment capacity of the beams.

TABLE III
RELATIVE IMPORTANCE RATIO ACCORDING TO GARSON FORMULA

Features	BPNN1 (5-3-1) %	BPNN2 (5-5-3-1) %
Width of the beam (b)	05	06
Effective depth (d)	44	42
Compression strength of concrete (f'c)	24	23
Ultimate tensile strength of re-bars (fu)	8	9
Reinforcement ratio (ρ)	19	20

V. PARAMETRIC STUDY

The most important benefit of creating models by the neural network is that it makes parametric study an easy job. Researchers can predict the influence of one factor by fixing all other factors. The parametric study focused on the carbon fiber polymer bars and glass fiber polymer bars which they are the common types mostly used. Parametric study has been done for BPNN2(5-5-3-1) model only which gains the higher correlation rate. The reason behind the difference in the accuracy of the two models is that BPNN2(5-5-3-1) model can save or remember higher numbers of relationships between nodes. It's an evident on the non-linearity relationships among influenced factors affecting the flexural strength of beams reinforced with FRP bars. 150 test samples are prepared (75 samples reinforced with carbon fiber polymer bars with fixed ultimate tensile strength (2300 MPa) and 75 samples reinforced with glass fiber polymer bars with fixed ultimate tensile strength (1000 MPa), all samples are high strength concrete (60 MPa, 80 MPa, 100 MPa)). Samples are fed to the BPNN2(5-5-3-1) model and moment capacity is predicted.

A. Parametric Study for Beams Reinforced with Carbon Fiber Polymer Bars

By using BPNN2(5-5-3-1) model, the flexural strength capacity of 75 concrete beams reinforced with carbon fiber polymer bars were predicted to evaluate the effect of parameters (effective depth, cylindrical concrete compressive strength and reinforcement ratio) on the flexural capacity of concrete beams reinforced with carbon fiber polymer bars.

Influence of Effective Depth

Effective depth is the most important parameter influencing the moment capability of a beam. Fig. 6 shows the BPNN2(5-5-3-1) neural network relationship between the effective depth

and moment capacity of the beam for different reinforcement ratios (0.15%, 0.30%, 0.45%, 0.60% and 0.75%).
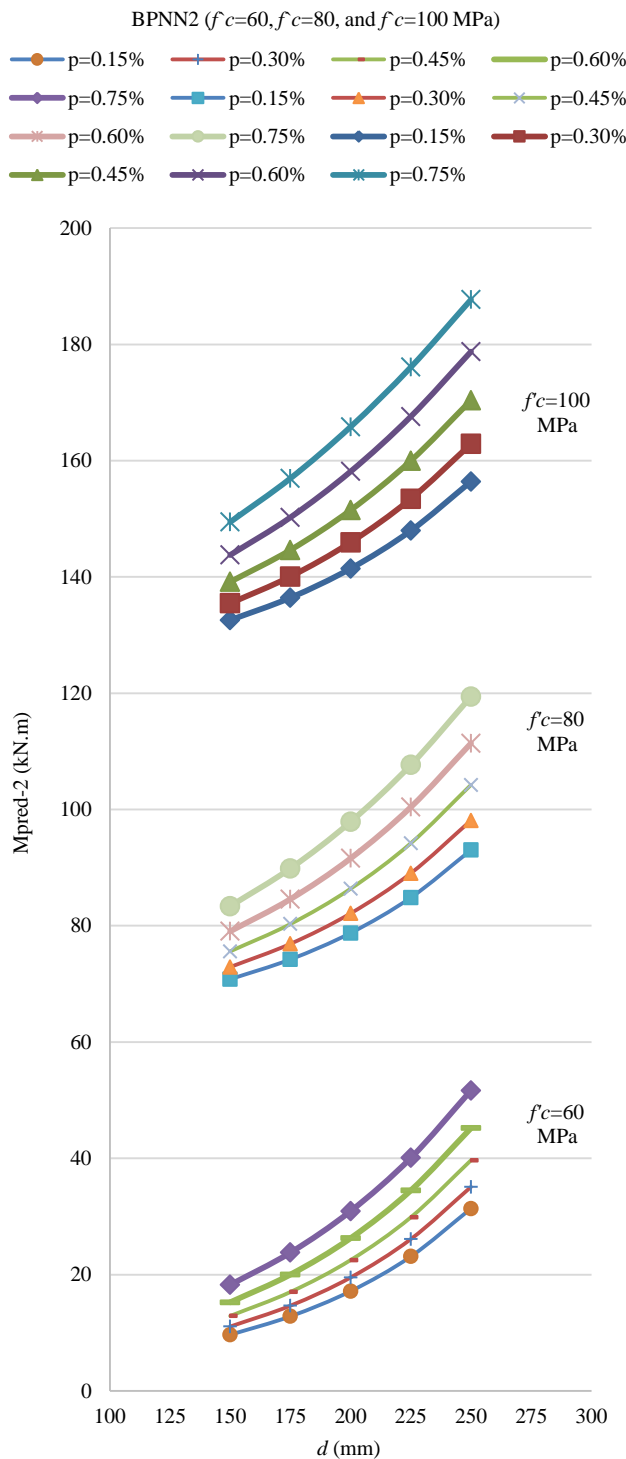
Fig. 6. Variation of the ultimate moment capacity with the effective depth and the reinforcement ratios.

In these relationships the ultimate tensile strength of the bars is already fixed to 2300 MPa, while the concrete strength is fixed to 60 MPa, 80 MPa and 100 MPa, different reinforcement ratio are used. Increasing the effective depth caused an increase in the moment capacity of beams with respect to the different reinforcement ratios. All curves look very normal and represent the realistic relationships of the effective depth and moment capacity.

A careful look to the three relationships in Fig. 6 shows that the slope of all curves being steeper when the effective depth of a beams increased. This means that the rate of increasing moment capacity is higher for beams having greater effective depth.

Influence of Compression Strength of Concrete

Fig. 7 is declaring the relationship between the cylindrical compressive strength of concrete and the predicted moment capacity of the beams. The relationships are created by fixing tensile strength of rebars to 2300 MPa as mentioned before and effective depth to (150 mm 175 mm, 200 mm, 225 mm, and 250 mm). Five curves are drawn for different reinforcement ratios (0.15%, 0.30%, 0.45%, 0.60% and 0.75%). By increasing the cylindrical compression strength, the sectional moment capacity will increase.

The slope of all curves in Fig. 7 increases with increase in the cylindrical compression strength of concrete (i.e. the rate of increase of the moment capacity when the concrete cylindrical compressive strength increased from 80 MPa to 100 MPa is greater than the rate of increase in the moment while the concrete compression strength increased from 60 MPa to 80 MPa). The increase in the moment capacity caused by increasing in reinforcement ratio is higher at 100 MPa concretes if compared with 60 MPa compression strengths.

Influence of Reinforcement Ratio

Fig. 8 shows the relationship between reinforcement ratio and predicted moment capacity of the beams. The Ultimate tensile strength of the bars is already fixed to 2300 MPa; different colored curves represent different concrete compressive strengths. The effective depths are (150 mm, 175 mm, 200 mm, 225 mm, and 250 mm) accordingly.

All curves in Fig. 8 look to be linear which means that the rate of increasing in moment capacity is constant, a small difference is sensible for green colored curves (100 MPa). The low compression strength concretes have flat slopes while higher compression strength concretes gives steeper gradient lines (i.e. increasing in the reinforcement ratio gives higher rates of increase in moment capacity for beams having higher concrete compressive strengths).

B. Parametric Study for Beams Reinforced with Glass Fiber Polymer Bars

Another set of 75 generated beams were used to represent the relationships among influenced factors for beams supposed to be reinforced with glass fiber polymer bars, BPNN2(5-5-3-1) is used to evaluate the effect of parameters (effective depth, cylindrical concrete compressive strength and reinforcement ratio) on the flexural capacity of concrete beams.
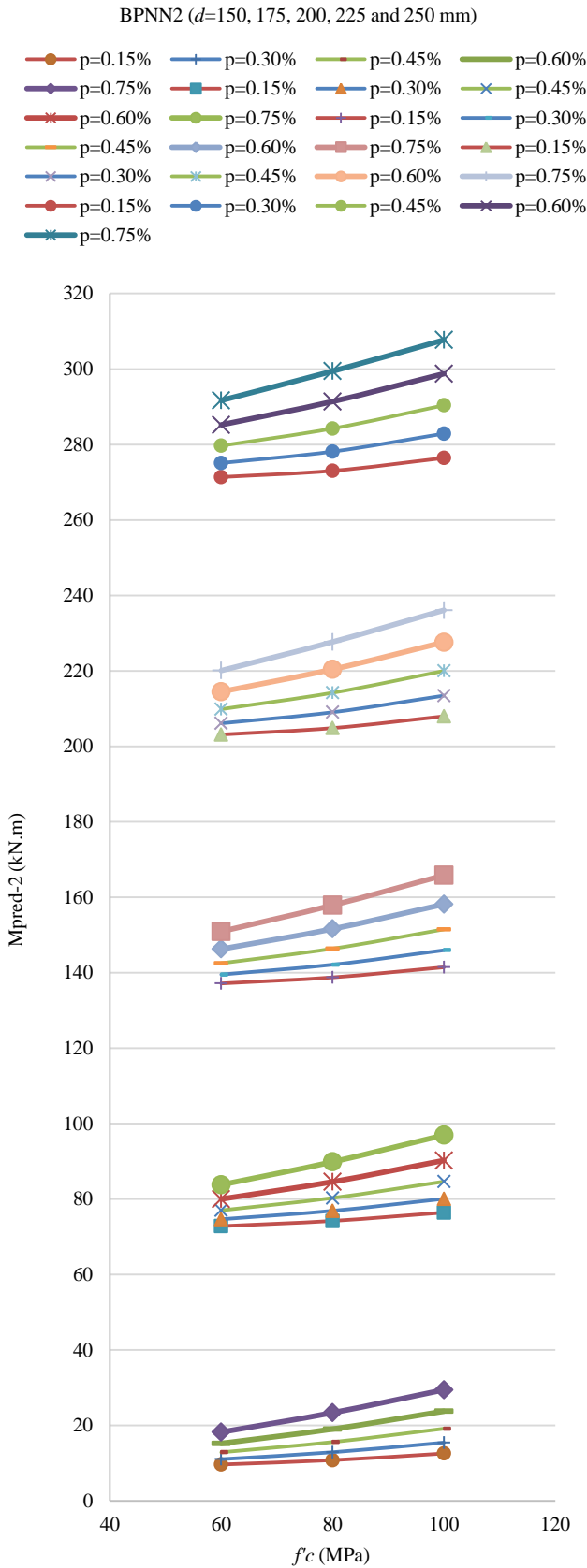
Fig. 7. Variation of the ultimate moment capacity with the cylindrical concrete compressive strength and the reinforcement ratios.
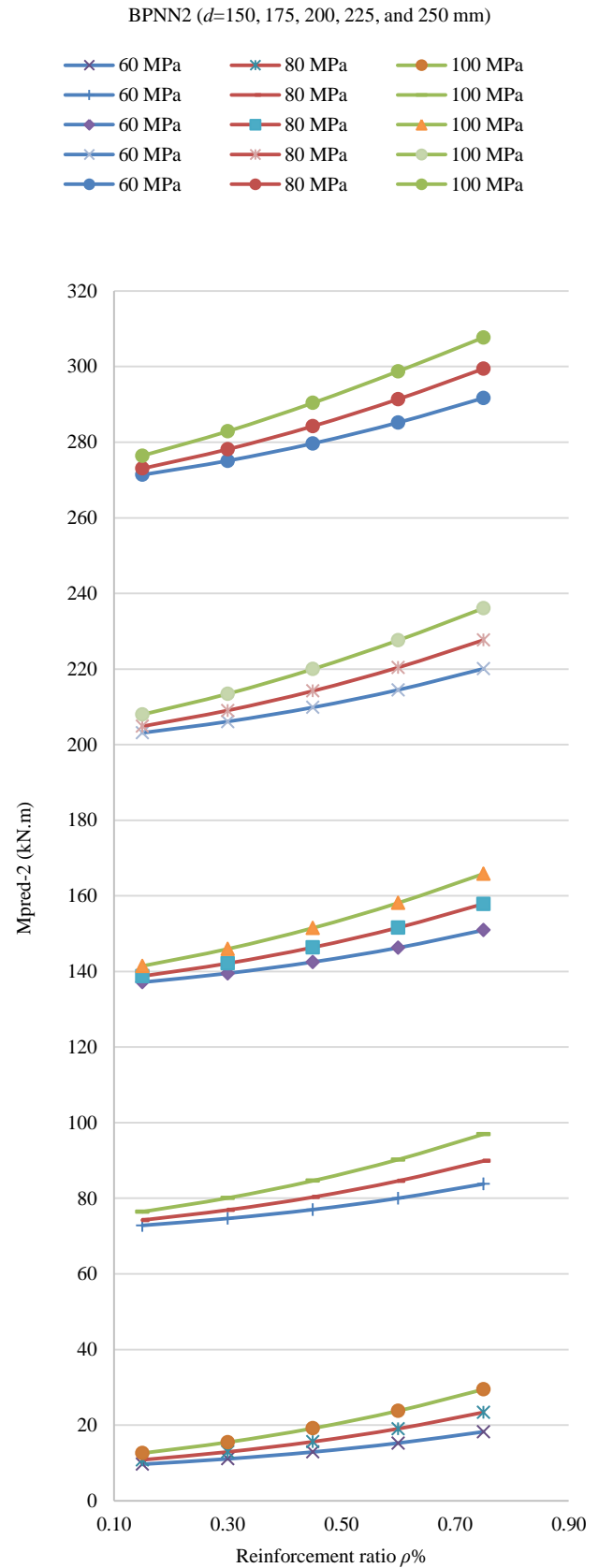
Fig. 8. Variation of the ultimate moment capacity with the reinforcement ratio and the cylindrical concrete compressive strengths.

Influence of Effective Depth

Fig. 9 shows the BPNN2(5-5-3-1) neural network relationship between the effective depth and the predicted moment capacity for beams having cylindrical concrete strengths 60 MPa, 80 MPa and 100 MPa respectively. Five curves are drawn representing the different reinforcement ratios (0.25%, 0.50%, 0.75%, 1.00% and 1.25%). The moment capacity of beams is increased by increasing the effective depth with respect to the different reinforcement ratios.

As shown in Fig. 9, the rate of increasing in moment capacity is higher in beams with greater effective depth (i.e. the slope of all curves being steeper when the effective depth of beams increased).

Influence of Compression Strength of Concrete

Fig. 10 shows the relationship between the cylindrical compressive strength of concrete and the predicted moment capacity of the beams. The relationships are created by fixing effective depth to 150 mm, 175 mm, 200 mm, 225 mm and 250 mm. Five curves are drawn for different reinforcement ratios (0.25%, 0.50%, 0.75%, 1.00% and 1.25%). By increasing the cylindrical compression strength, the sectional moment capacity will increase.

The rate of increase of the moment capacity when the concrete cylindrical compressive strength increased from 80 MPa to 100 MPa is greater than the rate of increase in the moment while the concrete compression strength increased from 60 MPa to 80 MPa (i.e., the slope of the curves increases with an increase in the cylindrical compression strength of concrete. The increase in the moment capacity caused by increasing in reinforcement ratio is higher at 100 MPa concretes if compared with 60 MPa concrete compressive strengths.

Influence of Reinforcement Ratio

Reinforcement ratio is one of the parameters that affecting the moment capability of a beams. Fig. 11 shows the BPNN2(5-5-3-1) neural network relationship between the reinforcement ratios and moment capacity of the beam for different concrete compressive strengths (60 MPa, 80 MPa and 100 MPa). In these relationships the ultimate tensile strength of the bars is already fixed to 1000 MPa (glass bar tensile strength), while the effective depth are 150 mm, 175 mm, 200 mm, 225 mm and 250 mm. Increasing the reinforcement ratio caused an increase in the moment capacity of beams with respect to the different concrete compression strengths.

After looking to the relationships in Fig. 11, it shows that the slope of all curves being steeper when the reinforcement ratios of a beams increased. This means that the rate of increasing moment capacity is higher for beams having greater reinforcement ratios. The amount of increasing in moment capacity obtained by increasing the concrete compressive strength at the reinforcement ratio 1.25% is greater than that obtained while the reinforcement ratio is 0.25% (i.e. Higher

amount of moment capacity obtained by increasing the concrete compressive strengths at high level of reinforcement ratios while smaller amount obtained by increasing the concrete strengths at small level of reinforcement ratios).
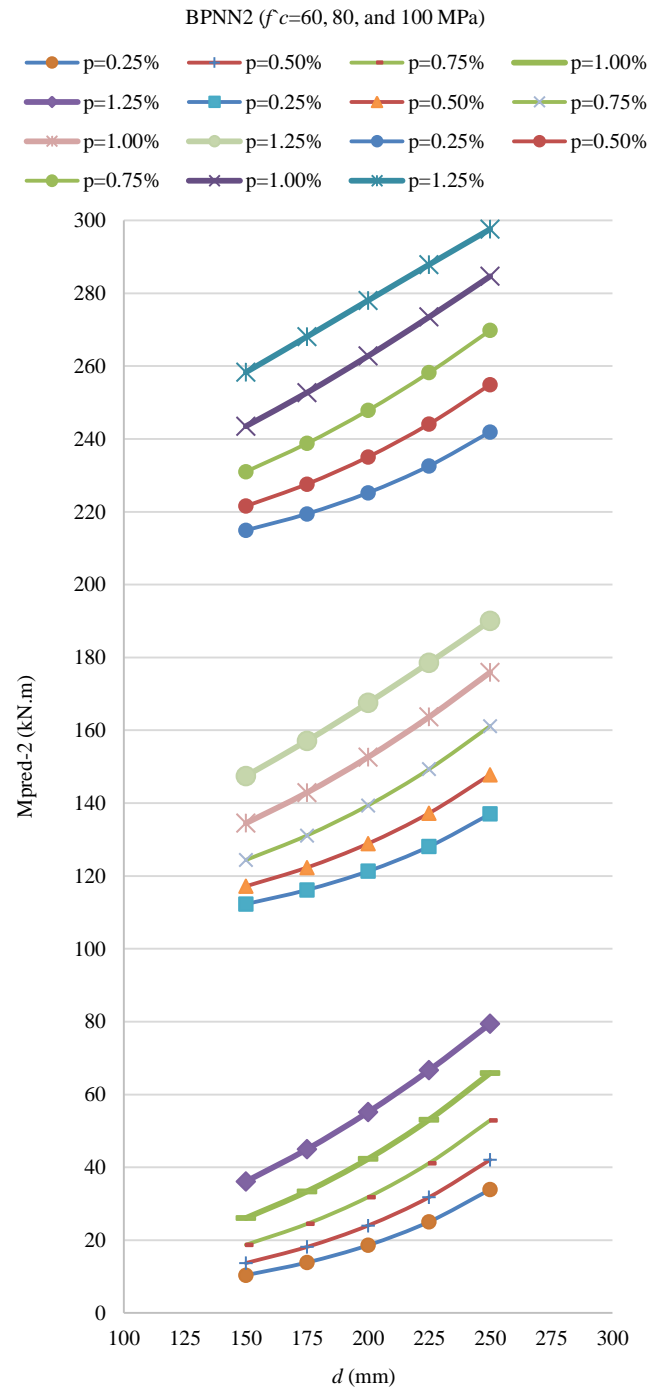
Fig. 9. Variation of the ultimate moment capacity with effective depth and reinforcement ratios.

VI. CONCLUSION

It is concluded that using a neural network model is successful in modeling the flexural behavior of beams reinforced with fiber reinforced polymer (FRP) bars.
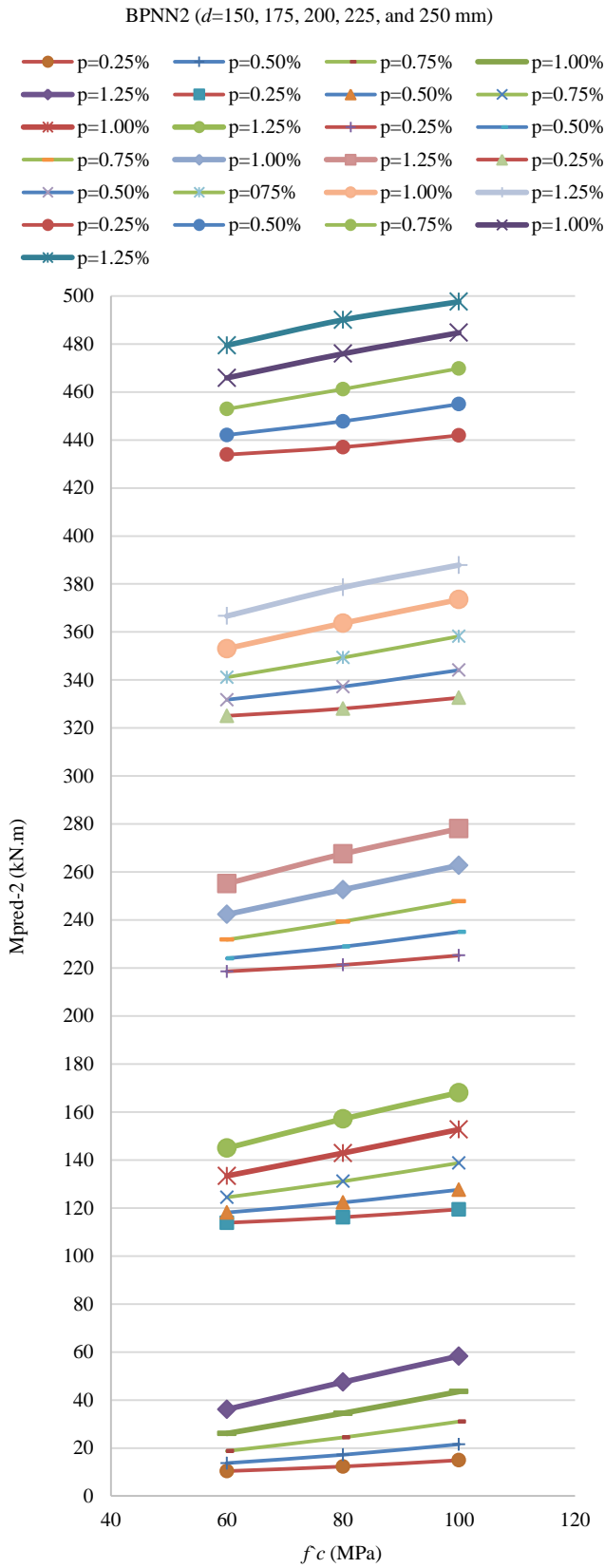
Fig. 10. Variation of the ultimate moment capacity with the cylindrical concrete compressive strength and the reinforcement ratios.
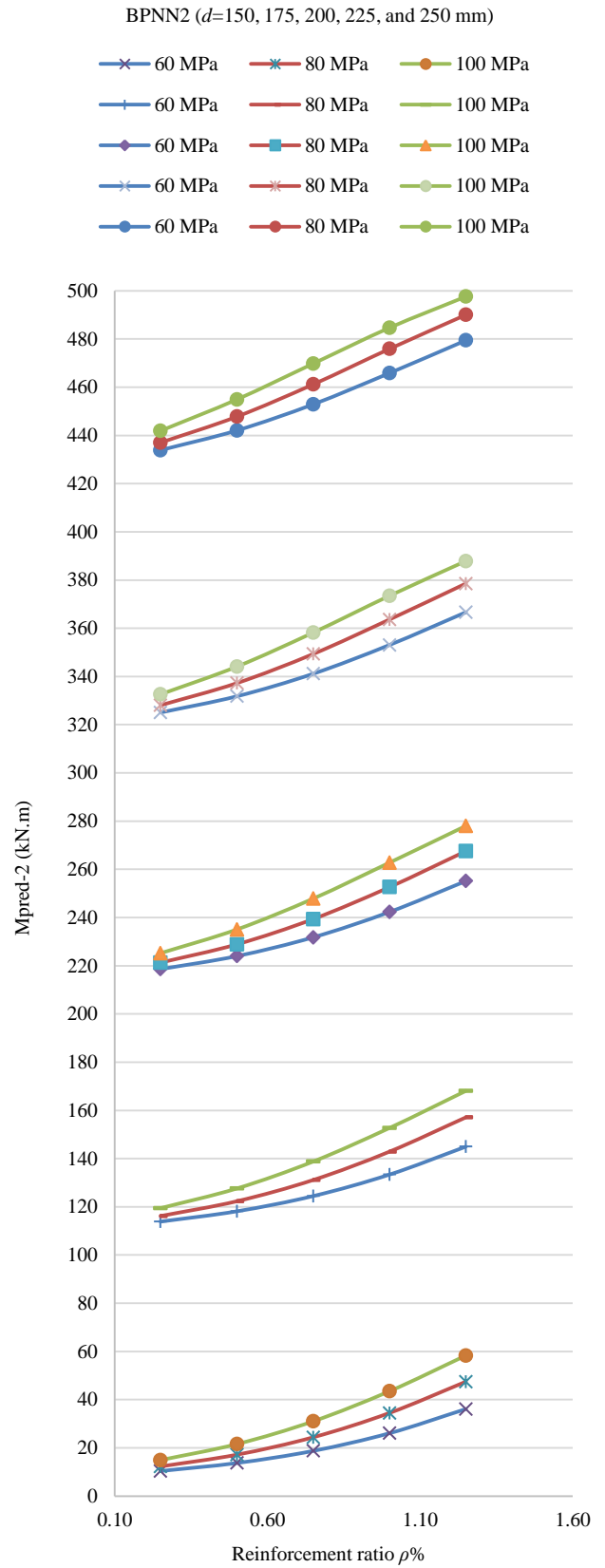
Fig. 11. Variation of the ultimate moment capacity with the reinforcement ratio and the cylindrical concrete compressive strengths.

The neural network with two hidden layers was more successful than the neural network with a single hidden layer in modeling the flexural behavior of beams reinforced with FRP bars which is evidence on the complex and high non-linearity of the relationships among influenced factors. The sigmoid transfer functions used in the hidden layers are acted successfully in the modeling process. Effective depth (*d*) has the largest effect among all other factors on the moment capacity of the beam, while width (*b*) has the least effect on the moment capacity of the beams. For data with high non-linearity such as reinforced concrete data "gradient descent with momentum" is a suitable back-propagation algorithm. The parametric study showed that the rate of increase in moment capacity of beams for higher levels of high strength concrete is much higher than the rate of increase in moment capacity of lower levels of high strength concrete beams.

APPENDIX A

SAMPLES COLLECTED FROM DIFFERENT SOURCES

No.	Beam notation	Source	b (mm)	d (mm)	f'c (MPa)	fu (MPa)	ρ%	Mexp (KN.m)
1	ISO2	(Benmoktane, et al., 1995)	200	259.00	43.00	690	1.10	80.40
2	ISO3		200	509.00	43.00	690	0.56	181.70
3	ISO4		200	509.00	43.00	690	0.56	181.70
4	CB2B-1	(Masmoudi, et al., 1998)	200	252.55	52.00	773	0.56	57.90
5	CB2B-2		200	252.55	52.00	773	0.56	59.80
6	CB3B-1		200	252.55	52.00	773	0.91	66.00
7	CB3B-2		200	252.55	52.00	773	0.91	64.80
8	CB4B-1		200	207.65	45.00	773	1.38	75.40
9	CB4B-2		200	207.65	45.00	773	1.38	71.70
10	CB6B-1		200	207.65	45.00	773	2.15	84.80
11	CB6B-2		200	207.65	45.00	773	2.15	85.40
12	GB1-1	(Toutanji and Saafi, 2000)	180	268.00	35.00	695	0.52	60.00
13	GB1-2		180	268.00	35.00	695	0.52	59.00
14	GB2-1		180	268.00	35.00	695	0.79	65.00
15	GB2-2		180	268.00	35.00	695	0.79	64.30
16	GB3-1		180	255.00	35.00	695	1.10	71.00
17	GB3-2		180	255.00	35.00	695	1.10	70.50
18	GB5	(Duranovic et al., 1997)	150	210.00	24.96	1000	1.31	40.31
19	GB9		150	210.00	31.84	1000	1.31	39.73
20	GB10		150	210.00	31.84	1000	1.31	39.50
21	GB13		150	210.00	34.72	1000	0.87	34.75
22	C-212-D1	(Barris, et al., 2009)	140	163.40	59.80	1000	0.99	36.90
23	C-216-D1		140	163.40	56.30	1000	1.78	44.04
24	C-316-D1		140	163.40	55.20	1000	2.67	50.16
25	C-212-D2		160	142.50	39.60	1000	0.99	26.61
26	C-216-D2		160	140.60	61.70	1000	1.78	41.31
27	C-316-D2		160	140.60	60.10	1000	2.67	45.18
28	NCF1	(Chitsazan, et al., 2010)	130	200.00	41.40	690	0.49	33.60
29	NCF2		100	170.00	41.40	690	0.75	23.99
30	NCF3		90	190.00	41.40	690	0.74	22.94
31	NCF4		80	160.00	41.40	690	0.99	17.16
32	NCF5		130	200.00	73.90	690	0.49	25.52
33	NCF6		100	170.00	73.90	690	0.75	21.67
34	NCF7		90	190.00	41.40	690	0.74	26.19
35	NCF8		80	160.00	41.40	690	0.99	18.09
36	BG1a	(Al-Sunna, 2006)	150	220.24	40.55	665	0.43	17.30
37	BG1b		150	220.24	40.55	665	0.43	17.10
38	BG2a		150	218.65	40.55	620	0.77	30.95
39	BG2b		150	218.65	40.55	620	0.77	29.84
40	BG3a		150	171.43	39.53	670	3.93	42.99
41	BG3b		150	171.43	39.53	670	3.93	45.02
42	BC1a		150	221.83	47.09	1450	0.29	28.26
43	BC1b		150	221.83	47.09	1450	0.29	29.53
44	BC2a		150	220.24	44.71	1325	0.65	40.19
45	BC2b		150	220.24	44.71	1325	0.65	39.58
46	BC3a		150	218.65	44.03	1475	1.16	47.09
47	BC3b		150	218.65	44.03	1475	1.16	47.78
48	SG1a		500	89.33	43.35	600	0.35	07.76
49	SG1b		500	89.33	43.35	600	0.35	06.83
50	SG2a		500	84.24	39.27	665	0.79	15.11
51	SG2b		500	84.24	39.27	665	0.79	16.88
52	SG3a		500	70.48	39.02	670	3.33	23.48
53	SG3b		500	70.48	39.02	670	3.33	23.78
54	SC1a		500	85.83	42.59	1450	0.28	14.25
55	SC1b		500	83.83	42.59	1450	0.28	14.06
56	SC2a		500	77.24	43.35	1325	0.63	21.11
57	SC2b		500	80.24	43.35	1325	0.63	21.26
58	SC3a		500	71.15	42.33	1475	1.14	22.99
59	SC3b		500	77.65	42.33	1475	1.14	26.70
60	G16L	(Al-Shamaa, 2010)	125	166.00	40.23	655	1.86	23.68
61	G12L		125	168.00	41.94	690	1.19	21.24
62	G10L		125	169.00	42.45	690	0.67	14.52
63	G6L		125	171.00	40.78	867	0.30	07.92
64	G10LH		125	169.00	47.56	690	0.67	15.04
65	G10LS		125	169.00	43.34	690	0.67	14.59
66	G12N		125	168.00	42.73	690	1.19	22.96
67	G10N		125	169.00	44.78	690	0.67	15.24
68	G6N		125	171.00	42.73	867	0.30	08.48
69	B10L		125	169.00	40.23	1127	0.74	15.28
70	B6L		125	171.00	39.56	1029	0.27	09.40
71	B10LH		125	169.00	46.75	1127	0.74	16.16
72	B10LS		125	169.00	41.92	1127	0.74	17.31
73	B10N		125	169.00	43.56	1127	0.74	17.88
74	B6N		125	171.00	40.59	1029	0.27	09.72
75	B1	(Taha, 2013)	100	126.50	62.77	2300	0.15	05.43
76	B2		100	126.50	62.77	2300	0.30	10.96
77	B3		100	126.50	62.77	2300	0.45	14.49
78	B4		100	126.50	84.55	2300	0.15	05.60
79	B5		100	126.50	84.55	2300	0.30	11.80
80	B6		100	126.50	84.55	2300	0.45	17.40
81	B7		100	126.50	97.96	2300	0.30	11.52
82	B8		100	126.50	97.96	2300	0.45	18.41
83	B9		100	116.50	97.96	2300	0.65	19.46
84	B10		100	126.50	63.78	2300	0.15	05.57

85	B11	100	126.50	63.78	2300	0.30	11.90
86	B12	100	126.50	63.78	2300	0.45	13.72
87	B13	100	126.50	86.22	2300	0.15	05.57
88	B14	100	126.50	86.22	2300	0.30	12.29
89	B15	100	126.50	86.22	2300	0.45	18.80
90	B16	100	126.50	100.55	2300	0.30	12.92
91	B17	100	126.50	100.55	2300	0.45	18.24
92	B18	100	116.50	100.55	2300	0.65	19.25
93	B19	100	126.50	64.09	2300	0.15	06.27
94	B20	100	126.50	64.09	2300	0.30	09.21
95	B21	100	126.50	64.09	2300	0.45	10.68
96	B22	100	126.50	86.70	2300	0.15	05.71
97	B23	100	126.50	86.70	2300	0.30	11.80
98	B24	100	126.50	86.70	2300	0.45	14.04
99	B25	100	126.50	100.82	2300	0.30	12.57
100	B26	100	126.50	100.82	2300	0.45	18.48
101	B27	100	116.50	100.82	2300	0.65	19.60

References

Al-Shamaa, M.F.K., 2010. *Behaviour of Lightweight Concrete Beams Reinforced with Fibre Reinforced Polymer Bars,* PhD. University of Technology Baghdad, Iraq.

Al-Sunna, R.A.S., 2006. *Deflection Behaviour of FRP Reinforced Concrete Flexural Members,* PhD. University of Sheffield.

Barris, C. et al., 2009. An experimental study of the flexural behaviour of GFRP RC beams and comparison with prediction models. *Composite Structures*, 91, pp.286-95.

Benmoktane, B., Chaallalt, O. and Masmoudi, R., 1995. Flexure Response of Concrete Beams Reinforced with FRP Reinforcing Bars. *ACI Structural Journal*, 9(2), pp.46-55.

Chitsazan, I., Kobraei, M., Jumaat, M.Z. and Shafig, P., 2010. An experimental study on the flexural behavior of FRP RC beams and a comparison of the ultimate moment capacity with ACI. *Civil Engineering and Construction Technology*, 1(2), pp.27-42.

Duranovic, N., Pilakoutas, K. and Waldron, P., 1997. Tests on Concrete Beams Reinforced with Glass Fiber Reinforced Plastic Bars. In *Third International Symposium on Non-metallic (FRP) Reinforcement for Concrete Structures*. Sapporo, Japan, 1997. Japan Concrete Institute.

Hall, M. et al., 2009. The WEKA Data Mining Software: An Update. *SIGKDD Explorations*, 11(1), pp.10-18. Available at: http://www.cs.waikato.ac.nz/~ml/weka/index.html .

Lee, S. and Lee, C., 2014. Prediction of shear strength of FRP-reinforced concrete flexural members without stirrups using artificial neural networks. *Engineering Structures*, 61, pp.99-112.

Leung, C.K.Y., Ng, M.Y.M. and Luk, H.C.Y., 2006. Empirical Approach for Determining Ultimate FRP Strain in FRP-Strengthened Concrete Beams. *Journal of Composites for Construction*, 10(2), pp.125-38.

Mashrei, M.A., Seracino, R. and Rahman, M.S., 2013. Application of artificial neural networks to predict the bond strength of FRP-to-concrete joints. *Journal of Construction and Building Materials*, 40, pp.812-21.

Masmoudi, R., Theriault, M. and Benmokrane, B., 1998. Flexural Behavior of Concrete Beams Reinforced with Deformed Fiber Reinforced Plastic Reinforcing Rods. *ACI Structural Journal*, 96(6), pp.665-76.

Metwally, I.M., 2013. Prediction of Punching Shear Capacities of Two-way Concrete Slabs Reinforced with FRP Bars. *HBRC Journal*, 9, pp.125-33.

Muhammad Ali, P.J., 2014. Predicting the Gender of the Kurdish Writers in Facebook. *Sulaimani Journal for Engineering Sciences*, 1(1), pp.18-28.

Muhammad Ali, P.J., Surameery, N.M.S., Yunis, A.M. and Abulrahman, L.S., 2013. Gender Prediction of Journalists from Writing Style Style. *Aro, the Scientefic Journal of Koya University*, 1(1), pp.22-28. Retrieved from http://dx.doi.org/10.14500/aro.10031.

Perera, R., Tarazona, D., Ruiz, A. and Martín, A., 2014. Application of artificial intelligence techniques to predict the performance of RC beams shear strengthened with NSM FRP rods. Formulation of design equations. *Journal of Composites: Part B*, 66, pp.162-73.

Taha, B.O., 2013. *Flexural Response of High Strength Concrete Beams Reinforced with CFRP Rebars,* PhD. University of Salahadeen, Erbil, Iraq.

Toutanji, H.A. and Saafi, M., 2000. Flexural Behavior of Concrete Beams Reinforced with Glass Fiber-Reinforced Polymer (GFRP) Bars. *ACI Structural Journal*, 97(5), pp.712-19.

Yousif, S.T. and Al-Jurmaa, M.A., 2010. Modeling of ultimate load for R.C. beams strengthened with Carbon FRP using artificial neural networks. *Al-Rafidain Engineering Journal*, 18(6), pp.28-41.